Four- and Five-coordinate Osmium(IV) Nitrides and Imides: Circumventing the 'Nitrido-Wall'

Josh Abbenseth, Sarah C. Bete, Markus Finger, Christian Volkmann, Christian Würtele and Sven Schneider*

Universität Göttingen, Institut für Anorganische Chemie, Tammannstraße 4, 37077 Göttingen, Germany.

Supporting Information Placeholder

ABSTRACT: Osmium nitride chemistry is dominated by osmium(VI) in octahedral or square-pyramidal coordination. The stability of the d^2 configuration and preference of the strong σ- and π-donor nitride for apical coordination is in line with the Gray-Ballhausen bonding model. In contrast, low-valent osmium(IV) or other d^4 nitrides are rare and only reported with lower coordination numbers (CN ≤ 4) thereby avoiding π-bonding conflicts of the nitride ligand with the electron rich metal center. We here report the synthesis of square-planar osmium(IV) nitride [Os^{IV}N(PNP)] (PNP = N(CHCHP*t*Bu$_2$)$_2$). From there, a square pyramidal isonitrile adduct could be isolated, which surprisingly features basal nitride coordination. Analysis of this five-coordinate d^4 nitride shows an unusual binding mode of the isonitrile ligand, which explains the preference of the weakest σ-donor and strongest π-acceptor isonitrile for apical coordination.

INTRODUCTION

The reactivity of transition metal nitride complexes was extensively studied due to their relevance for important transformations, such as nitrogen fixation or nitrogen group transfer.[1] Nitride ligands bound to early transition metal ions are generally susceptible to electrophilic attack. This nucleophilicity is attributed to the polarization of $M^{\delta+}\equiv N^{\delta-}$ π-bonding and is therefore attenuated along the transition series with dropping metal *d*-orbital energies. In this respect, group 8 nitrides apparently define a transition. Some high-valent osmium(VI) and iridium(V) nitride complexes exhibit reactivity that is attributed to nucleophilic attack at the nitride. For example, Mayer and coworkers demonstrated that the philicity of osmium(VI) nitrides can be tuned by subtle changes of the coordination environment,[2] enabling ambiphilic nitride reactivity in some rare cases. This multifaceted reactivity renders group 8 nitride chemistry particularly attractive.

Scheme 1. Qualitative *d*-orbital splitting for square-pyramidal Os^{VI} and square-planar Os^{IV} nitrides.

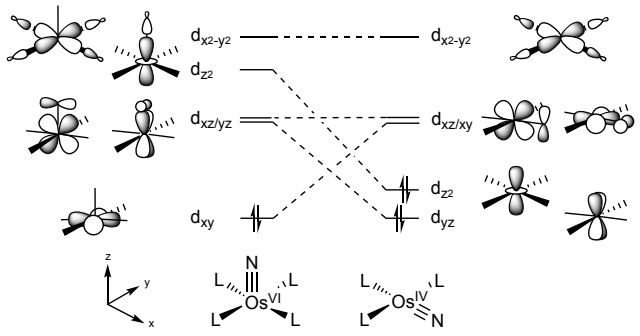

Scheme 2. Reported osmium(IV) nitrides (top) and PNP pincer ligands referred to in the text (bottom).

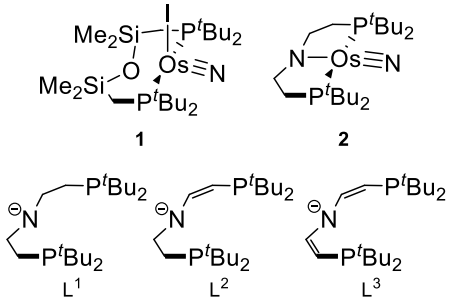

Besides the reactivity, group 8 also defines a border for M–N bonding. The Gray-Ballhausen (G-B) model rationalized transition-metal oxo bonding in the prevalent octahedral and square-pyramidal geometries.[3] This simple d-orbital splitting scheme can expanded to other two-faced π-donating, 6-electron donors, such as a terminal nitride (Scheme 1 left). Only one *d*-orbital remains σ- and π-nonbonding in character. Therefore, electronic configurations beyond d^2 are beyond the 'oxo/nitrido-wall' due to the destabilizing population of anti-bonding molecular orbitals (MOs). As a consequence, +VI is the dominating oxidation state for group 8 nitrido complexes.[1] In turn, isolable low-valent group 8 nitrides and terminal nitride complexes beyond group 8 are rare and generally exhibit lower coordination numbers, such as square-planar geometry, to evade π-bonding conflicts (Scheme 1 right).[4] For example, the only structurally characterized osmium(IV) nitrides **1** and **2** (Scheme 2) exhibit distorted tetrahedral (**1**) and square-planar coordination (**2**), respectively.[5,6]

Nitride **2** exhibits ambiphilic reactivity, as demonstrated by trimethylsilyl and trimethylphosphine addition to the nitride, respectively. However, the low coordination number gives rise to additional reaction patterns compared with 'traditional' nitride chemistry. For example, the reaction with Brønsted acid leads to reversible metal protonation and nitride hydrogenolysis affords the tetrahydride complex $[OsH_4(L^1)]$ (**3**) and ammonia in almost quantitative yield. In analogy to the respective ruthenium(IV) nitride,[7] this reaction presumably proceeds via initial H_2 heterolysis facilitated by pincer ligand cooperativity. As previously proposed by other groups,[8,9] these observations emphasize the relevance of low-valent group 8 nitrides for nitrogen fixation schemes. However, the reactivity of osmium(IV) nitrides generally remains scarcely examined.

In recent years, our group developed synthetic access to a series of dialkyl-, alkylvinyl- and divinylamido pincer complexes (Scheme 2).[10,11] Ligand backbone functionalization allows for tuning properties, such as ligand pK_a or redox potentials. These parameters are of particular importance for cooperative reactivity based on ligand centered hydrogen atom[12] or proton transfer.[13,14,15,16] Within the L^1–L^3 series, the fully oxidized ligand L^3 exhibits the lowest degree of N→M π-donation, and significantly enhanced chemical stability. We have utilized these features to control ground-state spin multiplicities[17,18] and stabilize unusual coordination geometries[19,20,21,22] or multiple bonding.[23,24,25] Recently Miller and co-workers also demonstrated that backbone dehydrogenation can also be coupled to nitride hydrogenolysis.[26] In this contribution, we expand the examination of low-valent group 8 nitrides. The use of the more robust pincer ligand L^3 allows for the unprecedented isolation of a five-coordinate osmium(IV) nitride, which lies beyond the 'nitrido-wall'.

RESULTS AND DISCUSSION

Synthesis of four-coordinate osmium(IV) nitride [OsN(L^3)]. The square-planar osmium(II) complex $[OsCl(L^3)]$ (**4**)[19] reacts with $[N(PPh_3)_2]N_3$ ([PPN]N_3) at room temperature as indicated by an immediate color change from purple to brown. From this reaction, the Os^{IV} nitride $[OsN(L^3)]$ (**5**) could be isolated in over 60% yield (Scheme 3). Intermediates were not observed suggesting rapid N_2-elimination after salt metathesis. Alternatively, **5** can also be generated via an Os(VI) nitride. The parent osmium(III) chloride $[OsCl_2(L^3)]$ (**6**)[19] gives $[Os^{VI}(Cl)N(L^3)]$ $[PF_6]$ (**7**) after azide salt metathesis and *in situ* oxidation with trityl salt in 68 % isolated yield (Scheme 3). Spectroscopic and crystallographic characterization of **7** (Figure 1) confirms the typical square pyramidal (τ = 0.14)[27] coordination geometry found for osmium(VI) with the nitride ligand in apical position. Treatment of **7** with an excess of Na/Hg allows for isolation of **5** in 95% yield.

Scheme 3. Synthesis of square-planar osmium(IV) nitride 5.

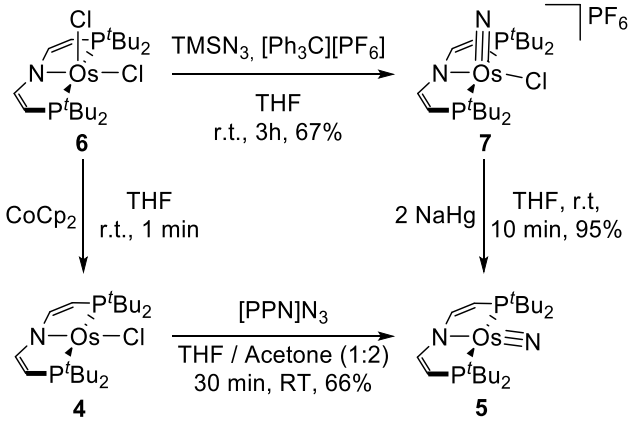

Multinuclear NMR characterization of diamagnetic **5** indicates C_{2v} symmetry on the NMR timescale at room temperature. However, the molecular structure in the solid state (Figure 1) features a distinctly bent Os≡N unit with respect to the pincer backbone (N1–Os1–N2: 152.8(2)). Such bending of the M≡N unit was also found for the previously reported osmium(IV) nitride **2**, albeit somewhat less pronounced (N-Os-N: 168.02(11)°), as well as for the ruthenium(IV) nitrides $[RuN\{N(SiMe_2CH_2PtBu_2)_2\}]$ (N-Ru-N: 155.86(13)°) and $[RuN(L^1)]$ (N-Ru-N: 165.6(3)°), respectively.[6,7,28] In fact, computational analysis of these compounds indicated very flat N–M–N bending potentials as a result of two mutually opposing effects: Bending of the strong donor ligand nitride out of the plane defined by the

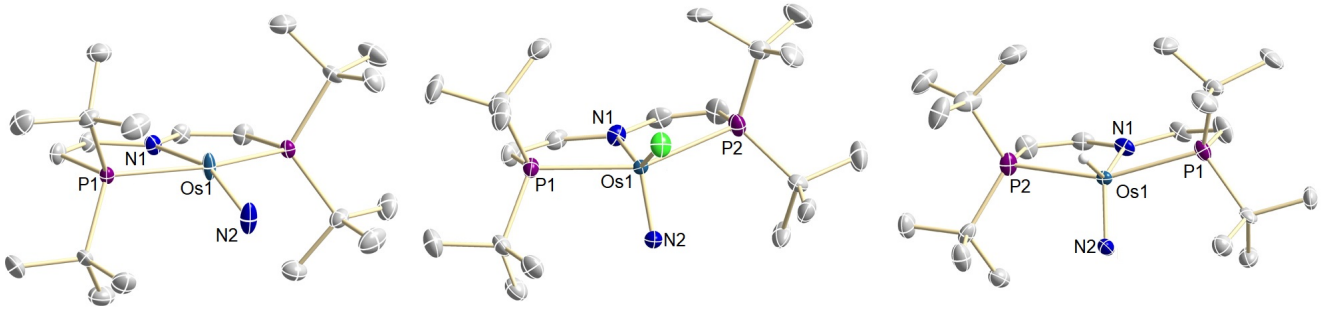

Figure 1. Molecular structure of complex **5** (left), **7** (center) and **8** (right) derived by single-crystal X-ray diffraction (thermal ellipsoids drawn at the 50% probability level); hydrogen atoms except the hydride ligand of **8** are omitted for clarity. Selected bond lengths [Å] and angles [°]: **5** Os1-N1 2.137(3), Os1-N2 1.735(5), Os1-P1 2.3697(7), N1-Os1-N2 152.8(2), P1-Os1-P1# 158.60(4); **7** Os1-Cl1 2.3277(18), Os1-N1 1.977(3), Os1-N2 1.629(4), Os1-P1 2.4400(12), Os1-P2 2.4408(11), N1-Os1-N2 107.55(19), P1-Os1-P2 155.35(4) , τ = 0.14; **8** Os1-H222 1.67(4), Os1-N1 2.029(3), Os1-N2 1.630(2), Os1-P1 2.4118(6), Os1-P2 2.4277(6), N2-Os1-H222 97.2(15), N1-Os1-H222 143.4(15), N1-Os1-N2 119.45(13), P1-Os1-P2 154.54(2), τ = 0.19.

pincer ligand stabilizes the HOMO with mainly d_{z2} character (Figure 2). In turn, the M≡N bond is slightly weakened due to reduced π-bonding, which is manifested by the longer nitride bond of **5** (1.735(5) Å) *vs.* more planar **2** (1.6832(18) Å). The Os≡N bond length of **5** is also considerably longer compared with osmium(VI) nitrides **7** (1.629(4) Å, see ESI) or [Os(H)N(L^3)]PF$_6$ (**8**; 1.60(2) Å, see below), respectively, attributed to the lower formal oxidation state and *trans*-influence of the pincer ligand.

Nitride hydrogenolysis. In previous work we demonstrated the hydrogenolysis of [MN(L^1)] (M = Ru, Os) with H_2 to give ammonia and polyhydride complexes in high yield.[6,7] Computational analysis for [RuN(L^1)] suggests metal-ligand cooperative H_2-heterolysis across the ruthenium amide bond as the initial step of the reaction sequence.[7] For the divinyl amide ligand L^3, not the amine nitrogen but the remote sp^2-carbon bound to phosphorous generally represents the basic pincer site.[12,20] Therefore, we examined nitride hydrogenolysis also for **5**. Exposure of **5** to H_2 (1 bar) at elevated temperatures results in clean conversion over 48 h with release of NH_3 in about 90 % yield (Scheme 4). Besides ammonia, the tetrahydride [Os(H)$_4$(HL^1)] (**3**) is obtained as in case of **2**.[6] The full hydrogenation of the oxidized ligand L^3 to parent amine HL^1 suggests cooperative H_2 activation also for the unsaturated ligand L^3.[11]

Scheme 4. Hydrogenolysis of 5 and reactions of 5 with electrophiles (Ar = C_6H_3-3,5-$(CF_3)_2$).

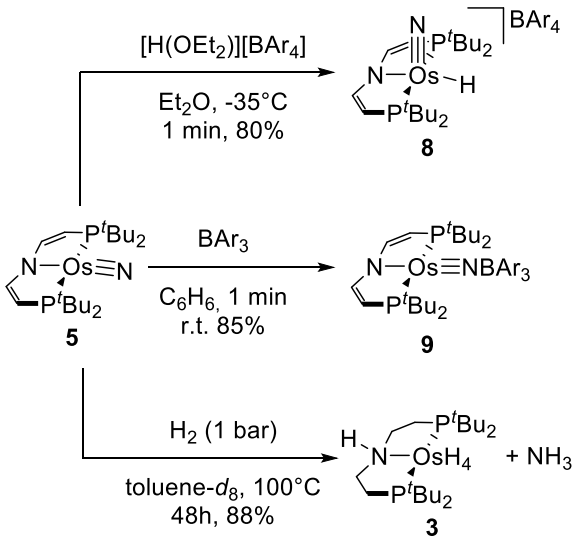

Reactivity of [OsN(L^3)] with electrophiles. The electron rich osmium(IV) nitride **5** readily reacts with electrophiles, such as Brønsted acids or boranes, respectively. In analogy to **2**, protonation results in electrophilic attack at the HOMO with mainly osmium d_{z2} character (Figure 2). Using Brookhart's acid, [H(OEt$_2$)$_2$][BArF$_{24}$] (BArF$_{24}^-$ = B(C$_6$H$_3$-3,5-(CF$_3$)$_2$)$_4^-$), [Os(N)H(L^3)][BArF$_{24}$] (**8**) can be isolated in

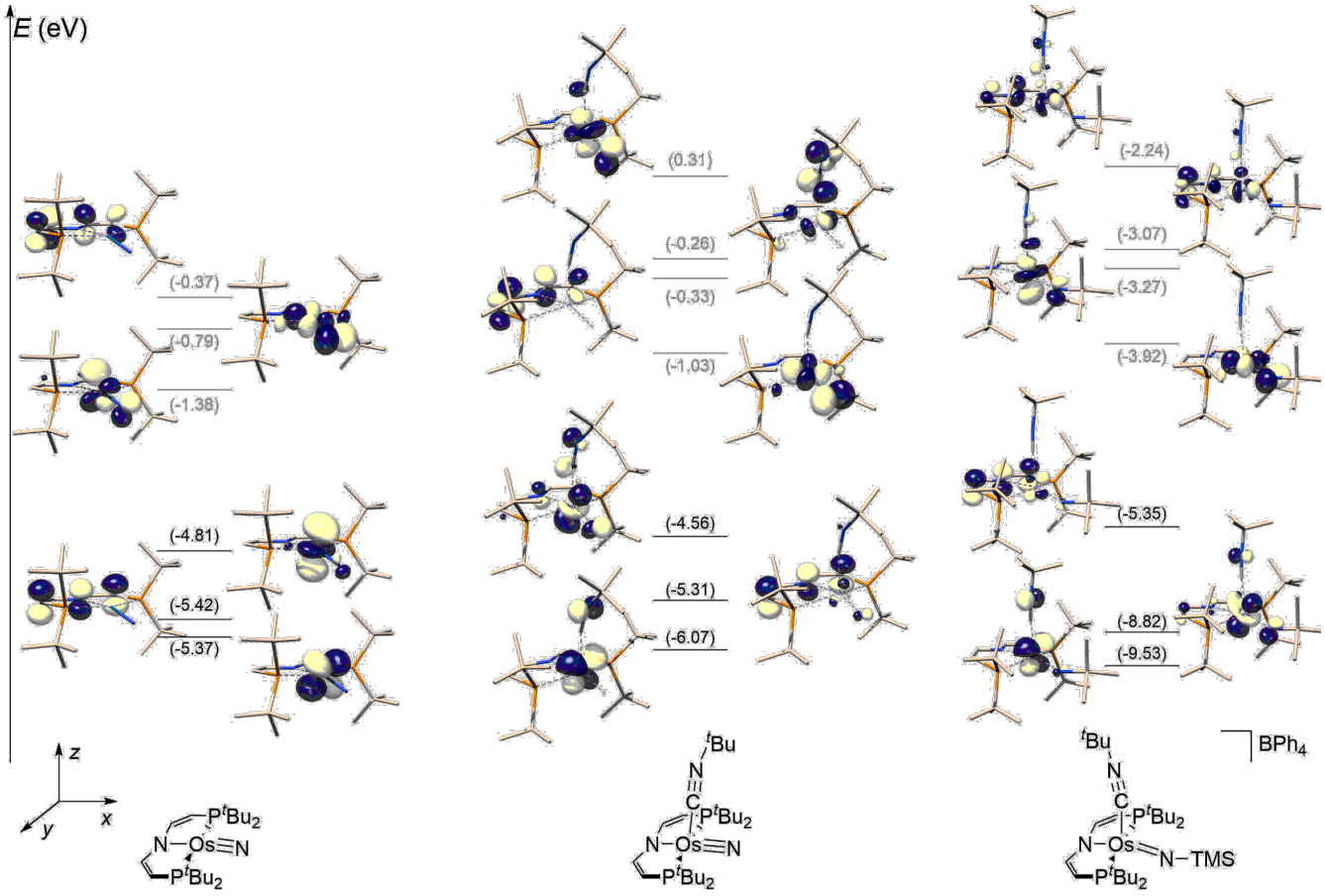

Figure 2. Computed (D3BJ-PBE0/def2-TZVP//D3BJ-RI-PBE/def2-SVP) molecular orbital (MO) scheme of compounds **5** (left) **10** (center) and **11** (right), respectively. Unoccupied MOs are drawn in grey, and MO energies given in eV.

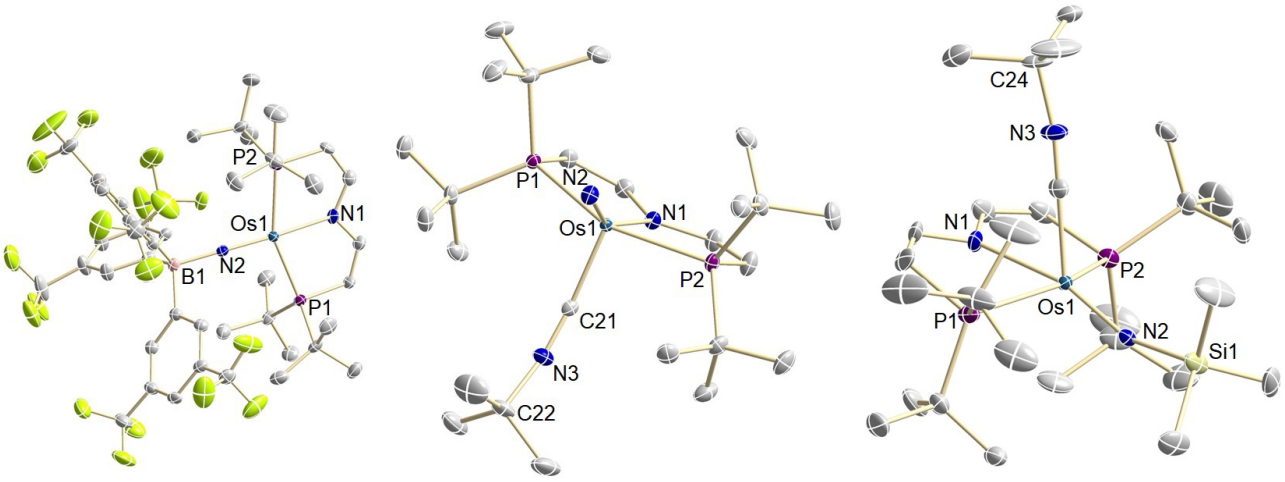

Figure 3. Molecular structure of complex **9** (left), **10** (center) and **11** (right) from single-crystal X-ray diffraction (thermal ellipsoids drawn at the 50 % (**9**, **10**) and 30 % (**11**) probability levels, respectively); hydrogen atoms are omitted for clarity. Selected bond lengths [Å] and angles [°]: **9** (one of two independent molecules) B1-N2 1.593(9), Os1-N1 2.087(5), Os1-N2 1.700(5), Os1-P1 2.4282(16), Os1-P2 2.3991(17), B1-N2-Os1 173.6(4), N1-Os1-N2 174.6(2), P1-Os1-P2 156.07(6); **10** (one of two independent molecules) C21-N3 1.175(3), Os1-C21 1.941(2), Os1-N1 2.2423(17), Os1-N2 1.6995(18), Os1-P1 2.4022(5), Os1-P2 2.4027(5), C21-N3-C22 160.7(2), N1-Os1-C21 91.25, N2-Os1-C21 116.05(9), N1-Os1-N2 152.69(8), P1-Os1-P2 150.970(18); **11** C24-N3 1.151(6), Os1-N1 2.237(4), Os1-N2 1.754(4), Os1-C24 1.933(5), Os1-P1 2.4169(12), Os1-P2 2.4232(13), C24-N3-C25 170.9(6), N1-Os1-C24 74.38(19), N2-Os1-C24 122.4(2), N1-Os1-N2 163.18(17), Os1-C24-N3 179.0(4), P1-Os1-P2 148.28(5), Os1-N2-Si1 156.8(3).

over 80% yield (Scheme 4). The hydride ligand of **8** was detected at δ = 0.47 ppm by ^{1}H-NMR spectroscopy. As expected for osmium(VI) square-pyramidal osmium coordination (τ = 0.19) is observed in the solid state (Figure 1) with the strong donor ligand nitride in apical position. The formal metal oxidation and the vacant site *trans* to the nitride result in decrease of the Os≡N bond length by more than 0.1 Å (Os1–N2: 1.60(2) Å) compared with **5**. In contrast to Brønsted acids, the sterically demanding Lewis acid $B(C_6H_3\text{-}3,5\text{-}(CF_3)_2)_3$ attacks the lone-pair of the nitride ligand (Scheme 4). The borane adduct [Os{NB(C_6H_3-3,5-$(CF_3)_2)_3$}(L^3)] (**9**) was isolated in over 80 % yield. Solution NMR characterization is in agreement with C_{2v} symmetry. The structure is further confirmed by single crystal X-ray analysis (Figure 3). The considerably reduced nitride bending of **9** (N1–Os1–N2: 174.6(2) / 176.7(2)°) compared with parent **5** is accompanied by slight shortening of the osmium nitride bond distance (Δ*d* = 0.03 Å). In contrast to **2**, which is selectively silylated at the nitride lone pair with $SiMe_3Br$,[6] the reaction of **5** with trimethylsilyl halides is surprisingly sluggish giving several products that could not be identified.

Reactivity with nucleophiles: synthesis of five-coordinate osmium(IV) nitride [OsN(CN*t*Bu)(L^3)]. Lewis acidic reactivity, such as the addition of a fifth ligand, might at first be anticipated for coordinatively unsaturated 16 valence-electron nitride complexes like **2** and **5**. However, five-coordinate d^4 nitrides are predicted to be unstable by the G-B model.[3,29] In fact, both **2**[6] and **5** (Figure 2, left) exhibit relatively high-lying LUMOs with mainly Os≡N π*-character suggesting weak electrophilicity. Accordingly, PMe_3 attacks at the nitride rather than the metal of **2** forming an equilibrium with the phosphoraneiminato complex [Os(N=PMe_3)(L^1)].[6] However, the addition of phosphines to nitrides is somewhat ambiguous due to the synergistic donor/acceptor character of phosphines in the transition state.[30] In contrast to **2**, complex **5** does not react with phosphines (PMe_3, PPh_3) or stronger nucleophiles like Grignard reagents. The apparently reduced electrophilicity of **5** *vs.* **2** correlates with a longer Os≡N bond and stronger bending of the nitride ligand. This observation suggests that reduced covalency in metal nitride bonding contributes to the shifted reactivity.

Scheme 5. Syntheses of five coordinate osmium(IV) nitrido and imido complexes.

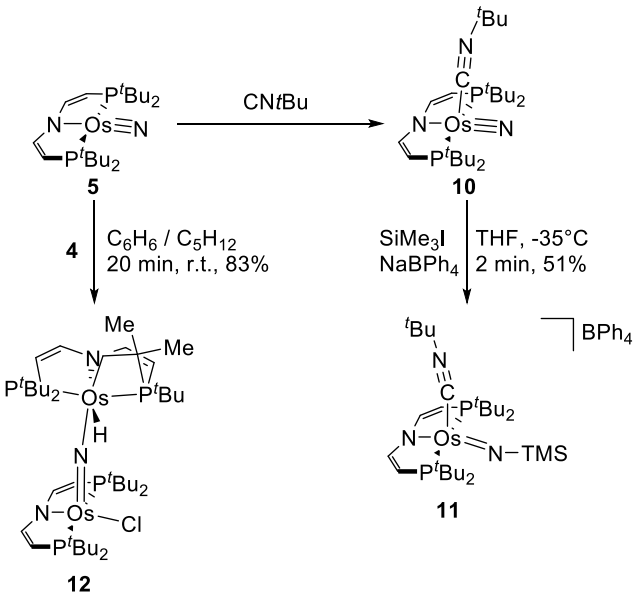

In contrast to phosphines, **5** immediately reacts with *tert*-butylisonitrile, even at low temperatures indicated by a color change from brown to bright green (Scheme 5). Surprisingly, NMR spectroscopic characterization at -50 °C

and single-crystal X-ray analysis (Figure 3) reveal the formation of an unprecedented five-coordinate osmium(IV) nitride, i.e. the thermally unstable complex [OsN(CN*t*Bu)(L^3)] (**10**). A particularly striking structural feature of square-pyramidal **10** (τ = 0.03) is the basal coordination of the nitride ligand. This contrasts with all other square-pyramidal nitrides which favor axial nitride coordination as a consequence of its strong *trans*-influence. Furthermore, the isonitrile ligand exhibits an unusual tilt expressed by the Os–C–N angle (165.16(8)/ 164.27(18)°). Marked bending within the isonitrile ligand (160.7(2)/154.9(2)°) and the distinct bathochromic shift of the C≡N stretching vibration ($\tilde{\nu}$ = 2007 cm^{-1}; nujol) support significant back-donation by the {OsN(L^3)}-platform. However, both values as well as the C≡N bond length (1.175(3)/1.180(3) Å) still favor the isonitrile (M–C≡N*t*Bu) over azavinylidene (M=C=N*t*Bu) resonance representation.[31,32] Interestingly, coordination of the isonitrile ligand keeps the nitride bond distance and angles almost unchanged (Os1-N2 1.6995(18), N1-Os1-N2 152.69(8)).

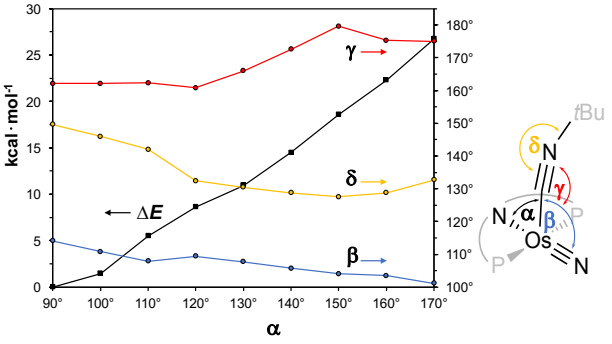

Figure 4. Relaxed surface scan for the (*t*BuNC)–Os–N$_{amide}$ angle (α) and selected structural parameters.

DFT computations were carried out to rationalize the stability and unusual structural features of complex **10**. The DFT model reproduces basal nitride and tilted isonitrile coordination (Os–C–N 162.1°). In fact, a local minimum for axial nitride coordination could not be found and a relaxed potential surface scan reveals a relatively steep energy surface that is around 25 kcal mol^{-1} above the ground state for such a structure (Figure 4). The computed frontier MO scheme of **10** (Figure 2, center) indicates considerable mixing of the metal in-plane interactions with the nitride and the isonitrile, respectively. A more localized bonding picture is provided by natural bond orbital (NBO) analysis (Scheme 6). The natural localized molecular orbital (NLMO) that represents the isonitrile/metal σ-interaction (Scheme 6b) reveals donation of the carbon lone pair into the metal d_{xz} orbital. The Os≡N antibonding character of this orbital results in a 3-center/4-electron interaction of the metal with the isocyanide (σ) and the nitride (π) ligand, respectively, besides the two cleanly defined 2c2e σ- and π-Os≡N bonds. However, this geometry also enables back-donation from the high-lying d_{z^2} orbital into the isonitrile π*-acceptor MO (Scheme 6c). Within this bonding picture, the isonitrile tilt is a consequence of avoiding an unfavorable σ-overlap with the filled d_{z^2} orbital but instead favorable back-donation from this orbital. Consequently, weak multicenter isonitrile σ-bonding results, which is counterbalanced by strong back-donation. Therefore, it is fully consistent that the weakest σ-donor and strong π-acceptor isonitrile coordinates apically, rather than the nitride ligand as in case of d^2 nitride complexes. These considerations suggest that such five-coordinate d^4 nitrides that are formally situated beyond the 'oxo-wall' can be stabilized with a weak σ-donor / strong π-acceptor ligand, such as isocyanide or CO.

Scheme 6. Qualitative MO-interaction diagram of the {Os(N)(PNP)}-platform with the isonitrile ligand (a; MO interactions depicted below marked in red) and NLMOs that represent the bonding σ- (b) and π- (c) and the antibonding σ-interaction (d) of the metal with the isonitrile.

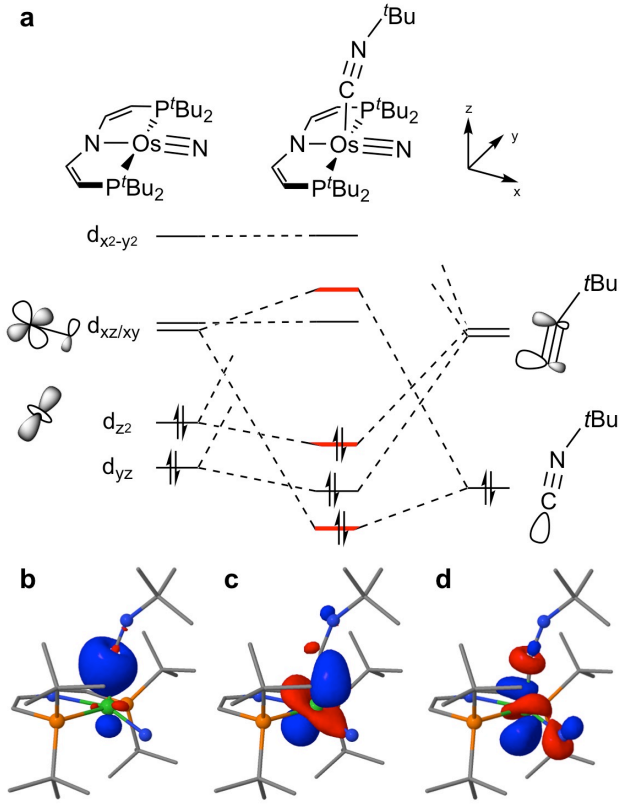

Synthesis of five-coordinate osmium(IV) imide [Os(NSiMe$_3$)(CN*t*Bu)(PNP)]$^+$. Compared with parent **5**, the five-coordinate nitride **10** exhibits much cleaner reactivity with silyl halide electrophiles. NMR spectroscopic monitoring reveals selective *in situ* nitride silylation with SiMe$_3$I. The silylimide complex [Os(NSiMe$_3$)(CN*t*Bu)(L^3)][BPh$_4$] (**11**) was isolated in around 50% yield after anion exchange with NaBPh$_4$ (Scheme 5). Contrary to nitride **10**, the five-coordinate osmium(IV) imido complex is thermally stable at room temperature both in solution and the solid state. Monomeric d^4 imido complexes are rare for the same general considerations discussed for nitrides.[33,34] Meyer and co-workers structurally characterized octahedral osmium(IV) imidos upon addition of cyanide, azide, amines or thiols to the respective osmium(VI) nitride.[35] Electron delocalization resulting from the heterocumulene character of these ligands probably contributes to their stability.

Furthermore, they exhibit distinct bending of the M=N–R moiety, which evades the in-plane π-bonding conflict with the low-valent metal center. In contrast, simple five- or six-coordinate d^4 alkyl-, aryl- or silylimides have not been characterized to date but might be intermediates in the addition of nucleophiles to electrophilic d^2 nitrides.[2,36]

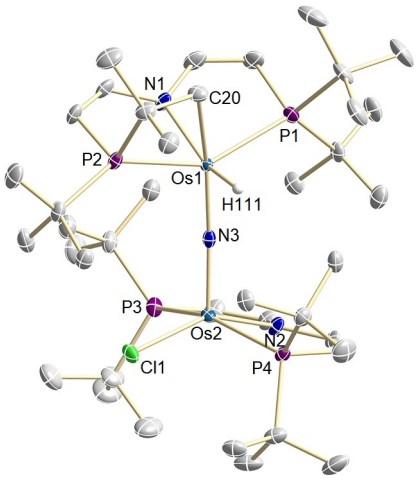

Figure 5. Molecular structure of complex **12** from single-crystal X-ray diffraction (thermal ellipsoids drawn at the 50 % probability level); hydrogen atoms except the hydride ligand are omitted for clarity. Selected bond lengths [Å] and angles [°]: **12** Os1-H111 1.53(4), Os1-N1 2.126(3), Os1-N3 1.839(3), Os1-C20 2.220(3), Os1-P1 2.3778(8), Os1-P2 2.4502(8), Os2-N2 2.034(4), Os2-N3 1.796(3), Os2-Cl1 2.3648(9), Os2-P3 2.4271(19), Os2-P4 2.4404(9); Os1-N3-Os2 170.11(16), P2-Os1-P1 150.09(3), P3-Os2-P4 155.95(4).

NMR spectroscopic characterization of **11** is in agreement with a C_s symmetric structure in solution. The molecular structure in the solid state (Figure 3) confirms slightly more distorted square-pyramidal geometry (τ = 0.25) compared with **10**. However, the overall relatively small structural perturbations that result from nitride silylation are reflected in the similarities of the computed frontier MO schemes (Figure 2). A distinct tilt of the isocyanide ligand is not observed for **11** (Os1-C24-N3 179.0(4)°) suggesting reduced $d_{z^2}\rightarrow\pi^*$(CN) back donation. This interpretation is supported by enhanced linearity of the isonitrile ligand (C24-N3-C25 170.9(6)°), a slightly shortened C≡N bond (C24-N3 1.151(6)Å) and a hypsochromic shift of the C≡N*t*Bu stretching vibration by about 120 cm^{-1} in the IR spectrum. Instead, the isocyanide ligand of **11** exhibits an incline towards the amide ligand (N1-Os1-C24 74.38(19)°) to maintain isonitrile σ-donation within the *t*BuNC–Os≡N σ/π 3c4e-interaction as detailed for **10**. Furthermore, bending of the imido moiety (Os1–N2–Si1 156.8(3)°) reduces the in-plane π-interaction of the metal with the nitride accompanied by lengthening of the Os1–N2 bond (1.754(4) Å). The unusual basal imide coordination is therefore once again attributed to a preference for the weakest σ-donor and strongest π-acceptor to coordinate apically.

Synthesis of nitride bridged osmium(IV/IV) complex [(L^3)ClOs(μ-N)OsH{N(CHCHP*t*Bu$_2$)(CHCHP*t*BuC-MeCH$_2$)}] (12). We recently reported the formation of nitride bridged diruthenium(II/IV) complexes [(L)Ru^{II}(μ-N)Ru^{IV}Cl(L)] (L = L^1, L^3).[37] The molecular structure of [(L^3)Ru(μ-N)RuCl(L^3)] indicates double bonding of the nitride with both Ru ions, reducing π-bonding conflicts of the low-valent metal ions with the nitride. The same arguments apply to the few other low-valent ruthenium[38] and osmium[39] μ-nitrido species. However, detailed bonding analysis is yet to be done.

The reaction of a freshly prepared solution of **4** with either equimolar amounts of **5** or 0.5 equiv. N_3SiMe_3 allows for the isolation of the bright green bridging nitride complex **12** (Scheme 5) after column chromatography in high yield. In contrast to the analogous ruthenium platform,[37] spectroscopic and crystallographic (Figure 5) characterization of **12** reveals cyclometallation of one of the P*t*Bu substituents resulting in an {Os^{IV}(μ-N)Os^{IV}} core, that is close to linearity (Os1-N3-Os2 170.11(16)°). The two Os-PNP fragments are twisted towards each other by about 90° as a result of the bulky phosphines. The bond lengths of the nitride with the two osmium ions differ slightly (Os1-N3 1.839(3) Å, Os2-N3 1.796(3) Å) presumably due to the *trans*-influence of the alkyl substituent. Computational examination supports the osmium(IV/IV) redox state assignment. NBO analysis features one π-bond of the bridging nitride with each osmium ion, which are orthogonal to each other (Scheme 7). Consequently, the nitride effectively serves as a single-faced π-donor or metalloimido 4-electron donor ligand for both {Os^{IV}(PNP)} fragments, respectively. As a result, the d^4 configuration is easily sustained for five- and six-coordinate geometry and the μ-nitrido ligand occupies the apical site of the square-pyramidal fragment.

Scheme 7. NBO representation of the osmium/nitride π-bonding interactions in 12.

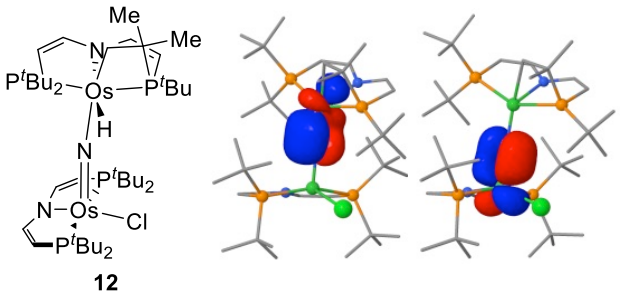

12

CONCLUSIONS

In summary, this paper exemplarily showcases different strategies to stabilize low-valent transition metal nitrido and imido complexes. Terminal nitrides of d^4-ions, such as osmium(IV) in square-pyramidal or octahedral geometry are formally beyond the 'nitrido-wall' defined by the G.-B. bonding model. Population of M–N π-antibonding MOs renders them inherently unstable. This π-conflict can be avoided by reduction of the coordination number. In analogy to osmium(IV), ruthenium(IV) and iridium(V) nitrides with bulky pincer ligands, the four-coordinate nitride complex **5** could be synthesized in high yield. Nucleophilic reactivity of the metal and the nitride is observed with Brønsted and Lewis acids, respectively. Nitride hydrogenolysis gives ammonia in high yield.

Surprisingly, the addition of *tert*-butylisocyanide allows for isolation of the five-coordinate, thermally labile osmium(IV) nitride **10**. The highly unusual preference of the isonitrile instead of the strong donor nitride for axial coordination is attributed to the high metal valence electron count and the unexpected binding mode of the isocyanide. Tilting about the Os–C–N angle allows on one hand for stabilization of the filled d_{z^2} orbital by π-back donation. On the other hand, mixing of the isonitrile lone pair with the in-plane Os≡N π-interaction results in an overall stabilizing 3c4e-interaction. This synergistic binding mode explains why the strong π-acceptor and comparatively weak σ-donor isocyanide is placed in the axial position. Nitride silylation further stabilizes this compound and allows for the first time for isolation of a d^4 silylimido complex beyond four-coordination. Electrophilic attack of low-valent nitrides provides a new synthetic route to such electron rich imidos. In analogy to the five-coordinate nitride **10**, 3c4e-bonding of the isonitrile in combination with reduced in-plane π-donation by imide bending stabilize silylimide **11**. Finally, stabilization arises from binding to two low-valent metal ions. The bridging nitride ligand within the {Os^{IV}=N=Os^{IV}} core of dinuclear complex **12** forms one π-bond with each osmium(IV) ion, respectively. The resulting Os–N double bond character also avoids π-bonding conflicts. Accordingly, the 'metallaimido' ligand is now in apical position of the OsCl(PNP) platform, as is usually observed for high-valent group 8 nitrido and imido complexes.

EXPERIMENTAL SECTION

All experiments were carried out using Schlenk (argon atmosphere) and glovebox (argon atmosphere) techniques. All solvents were dried by passing through columns packed with activated alumina. Deuterated solvents were obtained from Euriso-Top GmbH, dried over Na/K (THF, Toluene, Benzene) or CaH_2 (CD_2Cl_2) distilled by trap-to-trap transfer *in vacuo*, and degassed by three freeze–pump–thaw cycles, respectively. Silica gel 60 silanized was purchased from Merck KGaA and heated at 120°C *in vacuo* for 5 days prior to use. $CoCp_2$ (abcr), $[Ph_3C][PF_6]$, $[NBu_4][PF_6]$, CN*t*Bu, $B(C_6H_3\text{-}3,5\text{-}(CF_3)_2)_3$, N3SiMe3 (Sigma-Aldrich) and H_2 (Linde). $[OsCl_2(L^3)]$ and $[H(OEt_2)_2][B(C_6H_3\text{-}3,5\text{-}(CF_3)_2)_4]$ were prepared according to literature procedure.[19,40] IR spectra were recorded with a Thermo Scientific Nicolet iZ10 FT/IR spectrometer at room temperature. Elemental analyses were obtained from the analytical laboratories at the Georg-August University on an Elementar Vario EL 3. NMR Spectra were recorded on Bruker Avance III 300, Bruker Avance III 300, Bruker Avance III 400 and Bruker Avance III HD 500 and were calibrated to the residual solvent proton resonance. (d_6-Benzene d_H = 7.16 ppm, d_8-THF d_H = 3.58 ppm, d_8-toluene d_H = 2.08 ppm, CD_2Cl_2 = 5.32 ppm). LIFDI-spectrometry was performed on a Joel AccuTOF spectrometer under inert conditions. UV/vis measurements were recorded with an Agilent Technologies Cary 300 UV/vis spectrometer. Indophenolic titration was used for the quantification of ammonia.[41] Suitable single crystals for X-ray structure determination were selected from the mother liquor under an inert gas atmosphere and transferred in protective perfluoro polyether oil on a microscope slide. The selected and mounted crystals were transferred to the cold gas stream on the diffractometer. The diffraction data were obtained at 100 K on a Bruker D8 three-circle diffractometer, equipped with a PHOTON 100 CMOS detector and an INCOATEC microfocus source with Quazar mirror optics (Mo-Kα radiation, λ = 0.71073 Å). The data obtained were integrated with SAINT[42] and a semi-empirical absorption correction from equivalents with SADABS[43] was applied. The structure was solved and refined using the Bruker SHELX 2014 software package.[44] All non-hydrogen atoms were refined with anisotropic displacement parameters. All C-H hydrogen atoms were refined isotropically on calculated positions by using a riding model with their U_{iso} values constrained to 1.5 U_{eq} of their pivot atoms for terminal sp3 carbon atoms and 1.2 times for all other carbon atoms.

DFT calculations were carried out with the ORCA[45] program package using the PBE[46] and PBEo[47] functionals, respectively. Ahlrichs' basis sets def2-SVP (for geometry optimization and frequency calculation) and def2-TZVP (for single-point energies) were used with a full basis for all elements but Os for which the Stuttgart-Dresden 60 electron core potential was chosen to replace the inner shell 1s-4f orbitals.[48,49] The RI-J[50] (PBE) approximation in combination with the corresponding auxiliary basis sets of Alrichs was utilized to reduce computational costs in the geometry optimization and frequency calculations. Grimme's model (D3) with Becke-Johnson damping[51] was used to account for dispersion with the PBE or PBEo functionals. No symmetry restraints were imposed and the optimized structures were defined as minima (no negative eigenvalues) by vibrational analyses. NBO analysis of **5**, **10** and **12** was carried out with NBO 6.0.[52] Geometries were analyzed and visualized with Avogadro[53], molecular orbitals were visualized with Chimera[54] and for NBO/NLMO visualization, Jmol[55] was used.

Synthesis of [OsN(L^3)] (5). *Route A*: $[OsCl_2(L^3)]$ (85.5 mg, 138 µmol, 1.0 eq) and $CoCp_2$ (26.2mg, 138 µmol, 1.0 eq) are dissolved in THF (10 mL) and stirred for 1 minute under N_2 atmosphere. The solution is filtered into a solution of $[PPN]N_3$ (400 mg, 69 mmol, 5.0 eq) and stirred for 10 min. The solvent is removed and the residue is extracted with benzene (3 x 10 mL) and pentanes (10 x 5 mL). The solution is concentrated and cooled at -90°C for 16 h. The solution is filtered at -90°C and the residue is washed with pentane (2 x 5 mL). The product is extracted with benzene (3 x 3 mL) and lyophilization yields **5** as a brown powder (48.0 mg, 85.4 µmol, 62%).

Route B: Complex **7** (10 mg, 13.5 µmol, 1.0 eq) is dissolved in THF (5 mL). NaHg (620 mg, 0.1 w%, 27.0 µmol, 2.0 eq) is added and the solution is stirred for 5 minutes. After evaporation of the solvent the crude product is extracted with pentane (4 x 2 mL). [OsN(L^3)] (7.2 mg, 12.84 µmol, 95%) is obtained as a brown solid.

Anal. Calcd for $C_{20}H_{40}N_2OsP_2$ (560.73): C, 42.8; H, 7.19; N, 5.00 Found: C, 42.7; H, 7.13; N, 4.90. NMR (C_6D_6, RT): ^{1}H (400 MHz): δ = 6.99 (ABXX'B'A', $N = |^3J_{AX} + {}^4J_{AX'}| = 17.1$ Hz, $^3J_{AB}$ = 6.1 Hz. 2H, NC*H*), 4.56 (ABXX'B'A', $N = |^2J_{AX}+{}^4J_{AX'}| = 3.7$ Hz, $^3J_{AB}$ = 6.1 Hz, 2H, PC*H*), 1.54 ($A_{18}XX'A'_{18}$, $N = |^3J_{AX} + {}^5J_{AX'}| = 7.1$ Hz, 36H, P(C(CH_3)$_3$)$_2$). ^{13}C{^{1}H} (125.76 MHz): δ = 166.8 (AXX'A', $N = |^2J_{AX} + {}^3J_{AX'}| = 9.0$ Hz, 2C, N*C*H), 89.2 (AXX'A', $^1J_{CP}$ = 24.3 Hz. $^3J_{CP}$ = 22.6 Hz, 2C, PC*H*), 37.8 ($A_2XX'A'_2$, $N = |^1J_{AX} + {}^3J_{AX'}| = 12.7$ Hz, 4C, P(*C*(CH_3)$_3$)$_2$), 30.8 ($A_6XX'A'_6$, $N = |^2J_{AX} + {}^4J_{AX'}| = 2.9$ Hz, 12C, P(C(*C*H_3)$_3$)$_2$). ^{31}P{^{1}H} (161.25 MHz): δ = 81.2 (s, 2P, *P*(C(CH_3)$_3$)$_2$). MS (LIFDI, toluene): m/z = 562.1 (100%, [M$^+$]). IR (KBr): $\tilde{\nu}$ = 1025 (Os≡N).

Synthesis of [OsClN(L^3)][PF_6] (7). $[OsCl_2(L^3)]$ (100 mg, 162 µM, 1.00 eq) and $[Ph_3C][PF_6]$ (62.0 mg, 160 µM, 0.99 eq) are dissolved in THF (5 mL). $TMSN_3$ (21.2 µL, 160 µM, 0.99 eq) in THF (5 mL) is slowly added and the reaction is stirred for 3h. After evaporation of the solvent the crude product is washed with Et_2O (4 x 10 mL) and extracted with DCM (2 x 5 mL). The solution is layered with Et_2O (100 mL) and stored at -35°C for 16h. After filtration the residue is washed with Et_2O (2 x 5 mL) and extracted with DCM (2 x 5 mL). Evaporation of the solvent gives **7** as an orange powder (80 mg, 108µM, 67 %).

Anal. Calcd for $C_{20}H_{40}ClF_6N_2OsP_3$ (741.13): C, 32.4; H, 5.44; N, 3.77 Found: C, 32.6; H, 5.52; N, 3.70. NMR (CD_2Cl_2, RT): ^{1}H (500 MHz): δ = 7.76 (ABXX'B'A', $N = |^3J_{AX} + {}^4J_{AX'}| = 19.0$ Hz, $^3J_{AB}$ = 6.4 Hz. 2H, NC*H*), 5.09 (ABXX'B'A', $N = |^2J_{AX}+{}^4J_{AX'}| = 5.1$ Hz, $^3J_{AB}$ = 6.4 Hz, 2H,

PC*H*), 1.59 ($A_9XX'A'_9$, $N = |^3J_{AX} + {}^5J_{AX'}| = 8.5$ Hz, 18H, P(C(CH_3)$_3$)), 1.37 ($A_9XX'A'_9$, $N = |^3J_{AX} + {}^5J_{AX'}| = 8.3$ Hz, 18H, P(C(CH_3)$_3$)). $^{13}C\{^1H\}$ (125.76 MHz): $\delta = 170.0$ (AXX'A', $N = |^2J_{AX} + {}^3J_{AX'}| = 3.6$ Hz, 2C, N*C*H), 93.0 (AXX'A', $N = |^1J_{AX} + {}^3J_{AX'}| = 23.5$ Hz, 2C, PC*H*), 40.2 (AXX'A', $N = |^1J_{AX} + {}^3J_{AX'}| = 12$ Hz, 6C, P(*C*(CH_3)$_3$), 38.9 (AXX'A', $N = |^1J_{AX} + {}^3J_{AX'}| = 9.7$ Hz, 6C, P(*C*(CH_3)$_3$), 28.9 ($A_3XX'A'_3$, $N = |^2J_{AX} + {}^4J_{AX'}| = 1.8$ Hz, 6C, P(C(*C*H_3)$_3$), 28.9 (s br, 6C, P(C(*C*H_3)$_3$). $^{31}P\{^1H\}$ (161.25 MHz): $\delta = 91.5$ (s, 2P, *P*(C(CH_3)$_3$)$_2$), -145 (h, $^2J_{PF} = 711$ Hz, PF_6).

Synthesis of [OsHN(L^3)][BArF$_{24}$] (8). [OsN(L^3)] (5.0 mg, 8.9 µmol, 1.0 eq) is dissolved in Et_2O (2 mL) and cooled to -35°C. [H(Et_2O)$_2$][$BArF_{24}$] (9.0 mg, 8.9 µmol, 1.0 eq) is added and the solution is stirred for 10 min. The solvent is removed and the residue washed with pentanes (5 x 1 mL) and extracted with Et_2O (2 x 1 mL). The solvent is removed and **8** is isolated in form of a yellow solid (10 mg, 7.0 µmol, 80%).

Anal. Calcd for $C_{52}H_{53}BF_{24}N_2OsP_2$ (1242.96): C, 43.8; H, 3.75; N, 1.97 Found: C, 43.7; H, 3.83; N, 1.93. NMR (CD_2Cl_2, RT): ^1H (500 MHz): $\delta = 7.74$ - 7.71 (m, 8H, $C_{ortho}H$), 7.59 (ABXX'B'A', $N = |^3J_{AX} + {}^4J_{AX'}| = 19.0$ Hz, $^3J_{AB} = 6.3$ Hz. 2H, NC*H*), 7.58 – 7.55 (m, 4H, $C_{para}H$), 4.99 (ABXX'B'A', $N = |^2J_{AX} + {}^4J_{AX'}| = 5.3$ Hz, $^3J_{AB} = 6.3$ Hz, 2H, PC*H*), 1.49 ($A_9XX'A'_9$, $N = |^3J_{AX} + {}^5J_{AX'}| = 8.2$ Hz, 18H, P(C(CH_3)$_3$)), 1.26 ($A_9XX'A'_9$, $N = |^3J_{AX} + {}^5J_{AX'}| = 8.2$ Hz, 18H, P(C(CH_3)$_3$)), 0.47 (t, $^2J_{HP} = 13.5$ Hz, Os*H*). $^{13}C\{^1H\}$ (125.76 MHz): $\delta = 168.3$ (AXX'A', $N = |^2J_{AX} + {}^3J_{AX'}| = 5.3$ Hz, 2C, NCH), 162.3 (q, $^1J_{CB} = 49.8$ Hz, 4C, C_{ipso}), 135.3 (s, 8C, C_{ortho}), 129.4 (qq, $^2J_{CF} = 31.5$ Hz, $^3J_{CB} = 2.8$ Hz, 8C, C_{meta}), 125.1 (q, $^1J_{CF} = 272.4$ Hz, 8C, CF_3), 118.0 (h, $^3J_{CF} = 4.0$ Hz, 4C, C_{para}), 90.5 (AXX'A', $N = |^1J_{AX} + {}^3J_{AX'}| = 23.9$ Hz, 2C, PC*H*), 38.4 - 38.0 (m, 2C, P(*C*(CH_3)$_3$), 29.1 ($A_3XX'A'_3$, $N = |^2J_{AX} + {}^4J_{AX'}| = 1.8$ Hz, 6C, P(C(CH_3)$_3$), 28.9 ($A_3XX'A'_3$, $N = |^2J_{AX} + {}^4J_{AX'}| = 2.3$ Hz, 6C, P(C(CH_3)$_3$). $^{31}P\{^1H\}$ (161.25 MHz): $\delta = 101.5$ (s, 2P, *P*(C(CH_3)$_3$)$_2$).

Synthesis of [Os(NBArF$_{18}$)(L^3)] (9). [OsN(L^3)] (5.0 mg, 8.9 µmol, 1.0 eq) and $BArF_{18}$ (5.8 mg, 8.9 µmol, 1.0 eq) are dissolved in benzene (2 mL) and stirred for 5 minutes. The crude product is purified *via* column chromatography over silanized silica (benzene). Lyophilization yields **9** as a red powder (9.1 mg, 7.5 µmol, 85%).

Anal. Calcd for $C_{44}H_{49}BF_{18}N_2OsP_2$ (1210.85): C, 43.7; H, 4.08; N, 2.31 Found: C, 43.4; H, 3.90; N, 2.35. NMR (d_6-benzene, RT): ^1H (500 MHz): $\delta = 8.31 – 8.29$ (br, 6H, $C_{ortho}H$), 7.77 – 7.75 (br, 3H, $C_{para}H$), 5.69 (ABXX'B'A', $N = |^3J_{AX} + {}^4J_{AX'}| = 18.0$ Hz, $^3J_{AB} = 6.3$ Hz. 2H, NC*H*), 4.17 (ABXX'B'A', $N = |^2J_{AX} + {}^4J_{AX'}| = 4.4$ Hz, $^3J_{AB} = 6.3$ Hz, 2H, PC*H*), 1.04 ($A_{18}XX'A'_{18}$, $N = |^3J_{AX} + {}^5J_{AX'}| = 7.5$ Hz, 36H, P(C(CH_3)$_3$)). $^{13}C\{^1H\}$ (125.76 MHz): $\delta = 162.7$ (AXX'A', $N = |^2J_{AX} + {}^3J_{AX'}| = 8.6$ Hz, 2C, NCH), 147.3 (br, 1C, C_{ipso}), 135.9 (s, 6C, C_{ortho}H), 130.2 (q, $^2J_{CF} = 32.14$ Hz, 6C, C_{meta}H), 124.5 (q, $^1J_{CF} = 273.4$ Hz, 6C, CF_3), 120.4 (h, $^3J_{CF} = 4.0$ Hz, 3C, C_{para}H), 94.2 (AXX'A', $N = |^1J_{AX} + {}^3J_{AX'}| = 24.2$ Hz, 2C, PC*H*), 38.3 ($A_2XX'A'_2$, $N = |^1J_{AX} + {}^3J_{AX'}| = 12.0$ Hz, 4C, P(*C*(CH_3)$_3$)$_2$), 30.4 ($A_6XX'A'_6$, $N = |^2J_{AX} + {}^4J_{AX'}| = 2.4$ Hz, 12C, P(C(*C*H_3)$_3$)$_2$). $^{31}P\{^1H\}$ (161.25 MHz): $\delta = 82.7$ (s, 2P, *P*(C(CH_3)$_3$)$_2$.

Hydrogenolysis of [OsN(L^3)] (5). 5 (9.8 mg, 17.5 mmol, 1.0 eq) is dissolved in toluene-d_8 (0.5 mL) and heated to 100°C for 48 h under a dihydrogen atmosphere (1 bar). The reaction is followed by ^{31}P NMR spectroscopy with PPh_3O as internal standard (capillary). Ammonia was quantified by indophenolic titration.

Synthesis of [OsN(L^3)(CN*t*Bu)] (10). [OsN(L^3)] (20.4 mg, 36.1 µmol, 1.0 eq) and CN*t*Bu (4.3 mg, 37.9 µmol, 1.1 eq) are dissolved in thawing benzene (5 mL) and stirred for 10 s. The solvent is evacuated and [OsN(L^3)(CN*t*Bu)] is isolated in form of a green solid (23.1 mg, 36.1 µmol, quant.). ***10** is only stable at low temperatures (< -50°C) and cannot be stored as a solid without decomposition over the course of a few hours which prevented reproducible characterization by combustion analysis. Small amounts of benzene are still visible in the NMR spectra.*

NMR (d_8-THF, -50°C): ^1H (400 MHz): $\delta = 6.94$ (ABXX'B'A', $N = |^3J_{AX} + {}^4J_{AX'}| = 16.3$ Hz, $^3J_{AB} = 5.7$ Hz. 2H, NC*H*), 5.74 (ABXX'B'A', $N = |^2J_{AX} + {}^4J_{AX'}| = 4.2$ Hz, $^3J_{AB} = 5.7$ Hz, 2H, PC*H*), 1.51 (s, 9H, CN(C(CH_3)$_3$)), 1.40 ($A_9XX'A'_9$, $N = |^3J_{AX} + {}^5J_{AX'}| = 6.5$ Hz, 18H, P(C(CH_3)$_3$)), 1.34 ($A_9XX'A'_9$, $N = |^3J_{AX} + {}^5J_{AX'}| = 7.2$ Hz, 18H, P(C(CH_3)$_3$)). $^{13}C\{^1H\}$ (125.76 MHz): $\delta = 161.0$ (AXX'A', $N = |^2J_{AX} + {}^3J_{AX'}| = 7.3$ Hz, 2C, NCH), 155.9 (t, $^2J_{CP} = 3.2$ Hz, 1C, Os*C*), 82.2 (AXX'A', $N = |^1J_{AX} + {}^3J_{AX'}| = 26.2$ Hz, 2C, PC*H*), 57.4 (s, 1C, CN(*C*(CH_3)$_3$)$_2$), 38.1 (AXX'A', $N = |^1J_{AX} + {}^3J_{AX'}| = 13.6$ Hz, 2C, P(*C*(CH_3)$_3$), 37.9 (AXX'A', $N = |^1J_{AX} + {}^3J_{AX'}| = 11.3$ Hz, 2C, P(*C*(CH_3)$_3$), 32.3 (s, 3C, CC(*C*H_3)$_3$)$_2$), 31.6 – 31.4 (br, 12C, P(C(*C*H_3)$_3$)$_2$). $^{31}P\{^1H\}$ (161.25 MHz): $\delta = 73.3$ (s, 2P, *P*(C(CH_3)$_3$)$_2$). IR (nujol): $\tilde{\nu} = 2007$ (C=N).

Synthesis of [Os(NTMS)(L^3)(CN*t*Bu)][BPh$_4$] (11). [OsN(L^3)] (21.3 mg, 38.0 µmol, 1.0 eq) and $NaBPh_4$ (13.0 mg, 38.0 µmol, 1.0 eq) are dissolved in THF and CN*t*Bu (4.30 µL, 38.0 µmol, 1.0 eq) is added. The solution is stirred for 30 seconds and $SiMe_3I$ (4.92 µL, 38.0 µmol, 1.0 eq) is added. The solution is stirred for 2 minutes and the solvent is removed. The residue is washed with Et_2O and extracted with DCM. The extract is layered with pentanes and stored at -35°C for 16 h. After filtration the residue is washed with pentane (4 x 2 mL) and extracted with DCM (2 x 2 mL). **11** is isolated in form of an orange solid (20.1 mg, 19.4 µmol, 51%).

Anal. Calcd for $C_{52}H_{78}B_1N_3Os_1P_2Si$ (1036.29): C, 60.27; H, 7.59; N, 4.05 Found: C, 59.97; H, 7.25; N, 4.01. NMR (d_8-THF, -50°C): ^1H (500 MHz): $\delta = 7.34 – 7.29$ (m, 8H, $C_{meta}H$), 7.15 (ABXX'B'A', $N = |^3J_{AX} + {}^4J_{AX'}| = 18.3$ Hz, $^3J_{AB} = 5.8$ Hz. 2H, NC*H*), 7.05 – 7.00 (m, 8H, $C_{ortho}H$), 6.90 – 6.85 (m, 4H, $C_{para}H$), 4.33 (ABXX'B'A', $N = |^2J_{AX} + {}^4J_{AX'}| = 5.9$ Hz, $^3J_{AB} = 5.8$ Hz, 2H, PC*H*), 1.43 (s, 9H, CN(C(CH_3)$_3$)), 1.41 ($A_9XX'A'_9$, $N = |^3J_{AX} + {}^5J_{AX'}| = 7.7$ Hz, 18H, P(C(CH_3)$_3$)), 1.24 ($A_9XX'A'_9$, $N = |^3J_{AX} + {}^5J_{AX'}| = 7.8$ Hz, 18H, P(C(CH_3)$_3$)), 0.46 (s, 9H, Si(CH_3)$_3$). $^{13}C\{^1H\}$ (125.76 MHz): $\delta = 164.6$ (q, $^1J_{CB} = 49.0$ Hz, 4C, C_{ipso}), 161.1 (AXX'A', $N = |^2J_{AX} + {}^3J_{AX'}| = 5.5$ Hz, 2C, NCH), 136.4 (s, 8C, C_{meta}), 132.3 (br, 1C, Os*C*), 126.2 (q, $^2J_{CB} = 2.9$ Hz, 4C, C_{ortho}), 122.3 (s, 8C, C_{para}), 83.1 (AXX'A', $N = |^1J_{AX} + {}^3J_{AX'}| = 27.6$ Hz, 2C, PC*H*), 59.8 (s, 1C, CN(*C*(CH_3)$_3$)$_2$), 41.6 (AXX'A', $N = |^1J_{AX} + {}^3J_{AX'}| = 12.8$ Hz, 2C, P(*C*(CH_3)$_3$), 41.2 (AXX'A', $N = |^1J_{AX} + {}^3J_{AX'}| = 12.1$ Hz, 2C, P(*C*(CH_3)$_3$), 32.0 (s, 3C, CC(*C*H_3)$_3$)$_2$), 31.5 ($A_3XX'A'_3$, $N = |^2J_{AX} + {}^4J_{AX'}| = 1.7$ Hz, 6C, P(C(CH_3)$_3$), 29.5 ($A_3XX'A'_3$, $N = |^2J_{AX} + {}^4J_{AX'}| = 2.0$ Hz, 6C, P(C(CH_3)$_3$), 2.21 (s, 3C, Si(CH_3)$_3$). $^{31}P\{^1H\}$ (161.25 MHz): $\delta = 91.3$ (s, 2P, *P*(C(CH_3)$_3$)$_2$). IR (nujol): $\tilde{\nu} = 2128$ (C=N).

Synthesis of [(L^3)ClOs(µ-N)Os(H){N(CHCHP*t*Bu$_2$) (CHCHP*t*-BuCMeCH$_2$)}] (12). *Route A*: [$OsCl_2$(L^3)] (11.0 mg, 17.83 µmol, 1.0 eq) and $CoCp_2$ (3.4 mg, 17.83 µmol, 1.0 eq) are dissolved in benzene (5 mL) and stirred for 2 minutes at r.t. A solution of [OsN(L^3)] (10.0 mg, 17.83 µmol, 1.0 eq) in pentane (5 mL) is slowly added and the solution is stirred for 20 minutes at r.t. The solvent is removed and the residue extracted with pentanes (4 x 5 mL). The filtrate is concentrated and the crude product is purified *via* column chromatography with silanized silica (pentane). The solvent is removed and lyophilization yields **12** as a green powder (17.0 mg, 14.87 µmol, 83 %).

Route B: [$OsCl_2$(L^3)] (20.0 mg, 32.4 µmol, 1.0 eq) and $CoCp_2$ (6.2 mg, 32.4 µmol, 1.0 eq) are dissolved in benzene (5 mL) and stirred for 2 minutes. [TMS]N_3 (2.2 µL, 16.7 µmol, 0.5 eq) in pentane (5 mL) is slowly added and the solution is stirred for additional 20 minutes. The solvent is removed and the residue extracted with pentanes (4 x 5 mL). The filtrate is concentrated and the crude product is purified *via* column chromatography with silanized silica (pentane). The solvent is removed and lyophilization yields **12** as a green powder (13.2 mg, 11.5 µmol, 71%).

Anal. Calcd for $C_{40}H_{80}Cl_1N_3Os_2P_4$ (1142.9): C, 42.0; H, 7.06; N, 3.67 Found: C, 41.9; H, 6.94; N, 3.48. NMR (toluene- d_8, RT): ^1H (500 MHz): $\delta = 6.99$ (m, $^3J_{HH} = 6.1$ Hz, 1H, NC*H*), 6.89 (m, $^3J_{HH} = 6.0$ Hz, 1H, NC*H*), 6.67 (m, $^3J_{HH} = 6.3$ Hz, 1H, NC*H*), 6.61 (m, $^3J_{HH} = 6.3$ Hz, 1H, NC*H*), 4.44 (m, $^3J_{HH} = 6.0$ Hz, 1H, PC*H*), 4.34 (m, $^3J_{HH} = 6.3$ Hz, 1H, PC*H*), 4.31 (m, $^3J_{HH} = 6.1$ Hz, 1H, PC*H*), 4.18 (m, $^3J_{HH} = 6.3$ Hz, 1H, PC*H*), 1.93 – 1.07 (m, 69 H), 0.81 (m, 1H, OsCH_2), -0.56 (m, 1H, OsCH_2), -4.18 (m, 1H, Os*H*). $^{13}C\{^1H\}$ (125.76 MHz) $\delta = 168.5$ (dd, $^2J_{CP} = 10.3$ Hz, $^3J_{CP} = 2.7$ Hz, 1C, NCH), 168.4 (dd, $^2J_{CP} = 10.6$ Hz, $^3J_{CP}$

= 2.9 Hz, 1C, NCH), 162.4 (dd, $^2J_{CP}$ = 12.4 Hz, $^3J_{CP}$ = 2.0 Hz, 1C, NCH), 161.2 (dd, $^2J_{CP}$ = 10.1 Hz, $^3J_{CP}$ = 2.4 Hz, 1C, NCH), 93.9 (dd, $^1J_{CP}$ = 35.0 Hz, $^3J_{CP}$ = 2.5 Hz, 1C, PCH), 93.6 (d, $^1J_{CP}$ = 39.3 Hz, 1C, PCH), 93.2 (dd, $^1J_{CP}$ = 35.2 Hz, $^3J_{CP}$ = 1.7 Hz, 1C, PCH), 90.6 (d, $^1J_{CP}$ = 38.8 Hz, 1C, PCH), 58.1 (dd, $^1J_{CP}$ = 35.2 Hz, $^3J_{CP}$ = 5.4 Hz, 1C, P(*C*$(CH_3)_2CH_2Os$)), 39.1 (dd, $^1J_{CP}$ = 18.7 Hz, $^3J_{CP}$ = 2.7 Hz, 1C, P(*C*$(CH_3)_3$)), 38.1 (m, 2C, P(*C*$(CH_3)_3$)), 37.5 (dd, $^1J_{CP}$ = 13.9 Hz, $^3J_{CP}$ = 4.0 Hz, 1C, P(*C*$(CH_3)_3$)), 37.3 (dd, $^1J_{CP}$ = 13.2 Hz, $^3J_{CP}$ = 4.0 Hz, 1C, P(*C*$(CH_3)_3$)), 36.0 (dd, $^1J_{CP}$ = 13.9 Hz, $^3J_{CP}$ = 5.1 Hz, 1C, P(*C*$(CH_3)_3$)), 34.5 (dd, $^1J_{CP}$ = 6.6 Hz, $^3J_{CP}$ = 2.7 Hz, 1C, P(*C*$(CH_3)_3$)), 33.2 – 29.8 (21C), 32.3 (d, $^2J_{CP}$ = 3.6 Hz, 1C, P(C*C*$H_3)_2CH_2Os$)), 9.13 (dd, $^2J_{CP}$ = 30.4 Hz, $^2J_{CP}$ = 5.4 Hz, P(C$(CH_3)_2$*C*H_2Os)). $^{31}P\{^1H\}$ (202.46 MHz): δ = 38.0 (d, $^2J_{PP}$ = 250.2 Hz, 1P, *P*(C$(CH_3)_3$)), 19.7 (m, $^2J_{PP}$ = 291.6 Hz, $N = |^4J_{PP} + {}^4J_{PP}|$ = 2.5 Hz, 1P, *P*(C$(CH_3)_3)_2$), 16.6 (m, $^2J_{PP}$ = 291.6 Hz, $N = |^4J_{PP} + {}^4J_{PP}|$ = 2.5 Hz, 1P, *P*(C$(CH_3)_3)_2$), -15.5 (m, $^2J_{PP}$ = 250.1 Hz, $N = |^4J_{PP} + {}^4J_{PP}|$ = 2.5 Hz, 1P, *P*(C$(CH_3)_2CH_2Os$)). MS (LIFDI, toluene): m/z = 1143.5 (100%, $[M^+]$).

ASSOCIATED CONTENT

Supporting Information

The Supporting Information is available free of charge on the ACS Publications website.
Spectroscopic characterization of **5**, **7-12,** X-ray data for **5** and **7-12** and computational details of 5, **10-12.** (PDF)

AUTHOR INFORMATION

Corresponding Author

*sven.schneider@chemie.uni-goettingen.de

Notes

The authors declare no competing financial interest.

ACKNOWLEDGMENT

The authors are grateful to the European Research Council (ERC Grant Agreement 646747) and the Fond der Chemischen Industrie (FCI Doktoranden Stipendium for J.A.) for financial support.

REFERENCES

[1] (a) Eikey, R. A.; Abu-Omar, M. M. *Coord. Chem. Rev.* **2003**, *243*, 83-124. (b) Smith, J. M. *Progr. Inorg. Chem.* **2014**, *58*, 417-421.
[2] (a) Crevier, T. J.; Mayer, J. M. *J. Am. Chem. Soc. 1998*, **120**, 5595-5596 (b) Crevier, T. J.; Bennett, B. K.; Soper, J. D.; Bowman, J. A.; Dehestani, A.; Hrovat, D. A.; Lovell, S.; Kaminsky, W.; Mayer, J. M. *J. Am. Chem. Soc.* **2001**, *123*, 1059-1071.
[3] (a) Ballhausen, C. J.; Gray, H. B. *Inorg. Chem.* **1962**, *1*, 111-122. (b)Winkler, J. R.; Gray, H. B. *Struct. Bonding (Berlin)* **2011**, *142*, 17-28.
[4] Scheibel, M.; Abbenseth, J.; Kinauer, M.; Heinemann, F. W.; Würtele, C.; de Bruin, B.; Schneider, S. *Inorg Chem* **2015**, *54*, 9290-9302.
[5] Tsvetkov, N.; Pink, M.; Fan, H.; Lee, J.-H.; Caulton, K. G. Eur. J. *Inorg. Chem.* **2010**, *2010*, 4790-4800.
[6] Schendzielorz, F. S.; Finger, M.; Volkmann, C.; Würtele, C.; Schneider, S. *Angew. Chem. Int. Ed.* **2016**, *55*, 11417-11420.
[7] Askevold, B.; Nieto, J. T.; Tussupbayev, S.; Diefenbach, M.; Herdtweck, E.; Holthausen, M. C.; Schneider, S. *Nature Chem.* **2011**, *3*, 532-537.
[8] Kunkely, H.; Vogler, A. *Angew. Chem. Int. Ed.* **2010**, *49*, 1591-1593.
[9] Konnick, M. M.; Bischof, S. M.; Ess, D. H.; Periana, R. A.; Hashiguchi, B. G. *J. Mol. Catal. A Chem.* **2014**, *382*, 1-7.
[10] Schneider, S.; Meiners, J.; Askevold, B. *Eur. J. Inorg. Chem.* **2012**, *2012*, 412-429.
[11] Friedrich, A.; Drees, M.; Käss, M.; Herdtweck, E.; Schneider, S. *Inorg. Chem.* **2010**, *49*, 5482-5494.
[12] Schneck, F.; Finger, M.; Tromp, M.; Schneider, S. *Chem. Eur. J.* **2017**, *23*, 33-37.
[13] Silantyev, G. A.; Förster, M.; Schluschaß, B.; Abbenseth, J.; Würtele, C.; Volkmann, C.; Holthausen, M. C.; Schneider, S. *Angew. Chem. Int. Ed.* **2017**, *56*, 5872-5876.
[14] Marziale, A. N.; Friedrich, A.; Klopsch, I.; Drees, M.; Celinski, V. R.; Schmedt auf der Günne, J.; Schneider, S. *J. Am. Chem. Soc.* **2013**, *135*, 13342-13355.
[15] Glüer, A.; Förster, M.; Celinski, V. R.; Schmedt auf der Günne, J.; Holthausen, M. C.; Schneider, S. *ACS Catal.* **2015**, *5*, 7214-7217.
[16] Schiwek, C.; Meiners, J.; Förster, M.; Würtele, C.; Diefenbach, M.; Holthausen, M. C.; Schneider, S. *Angew. Chem. Int. Ed.* **2015**, *54*, 15271-15275.
[17] Askevold, B.; Khusniyarov, M. M.; Herdtweck, E.; Meyer, K.; Schneider, S. *Angew. Chem. Int. Ed.* **2010**, *49*, 7566-7569.
[18] Askevold, B.; Khusniyarov, M. M.; Kroener, W.; Gieb, K.; Müller, P.; Herdtweck, E.; Heinemann, F. W.; Diefenbach, M.; Holthausen, M. C.; Vieru, V.; Chibotaru, L. F.; Schneider, S. *Chem. Eur. J.* **2015**, *21*, 579-589.
[19] Abbenseth, J.; Diefenbach, M.; Bete, S. C.; Würtele, C.; Volkmann, C.; Demeshko, S.; Holthausen, M. C.; Schneider, S. *Chem. Commun.* **2017**, *53*, 5511-5514.
[20] Lagaditis, P. O.; Schluschaß, B.; Demeshko, S.; Würtele, C.; Schneider, S. *Inorg. Chem.* **2016**, *55*, 4529-4536.
[21] Meiners, J.; Scheibel, M. G.; Lemøe-Cailleau, M.; Mason, S. A.; Boeddinghaus, M. B.; Fässler, T. F.; Herdtweck, E.; Khusniyarov, M. M.; Schneider, S. *Angew. Chem. Int. Ed.* **2011**, *50*, 8184-8187.
[22] Kinauer, M.; Scheibel, M. G.; Abbenseth, J.; Heinemann, F. W.; Stollberg, P.; Würtele, C.; Schneider, S. *Dalton Trans.* **2014**, *43*, 4506-4513.
[23] Scheibel, M. G.; Wu, Y.; Stückl, A. C.; Krause, L.; Carl, E.; Stalke, D.; de Bruin, B.; Schneider, S. *J. Am. Chem. Soc.* **2013**, *135*, 17719-17722.
[24] Scheibel, M. G.; Askevold, B.; Heinemann, F. W.; Reijerse, E. J.; de Bruin, B.; Schneider, S. *Nature Chem.* **2012**, *4*, 552-558.
[25] Abbenseth, J.; Finger, M.: Würtele, C.; Kasanmascheff, M.; Schneider, S. *Inorg. Chem. Front.* **2016**, *3*, 469-477.
[26] Lindley, B. M.; Bruch, Q. J.; White, P. S.; Hasanayn, F.; Miller, A. J. M. *J. Am. Chem. Soc.* **2017**, *139,* 5305-5308.
[27] Addison, A. W.; Rao, T. N.; Reedijk, J.; van Rijn J., Verschoor, G. C. *J. Chem. Soc., Dalton Trans.* **1984**, 1349-1356.
[28] Walstrom, A.; Pink, M.; Yang, X.; Tomaszewski, J.; Baik, M.; Caulton, K. G. *J. Am. Chem. Soc.* **2005**, *127*, 5330-5331.
[29] Gloaguen, Y.; Rebreyend, C.; Lutz, M.; Kumar, P.; Huber, M.; van der Vlugt, J. I.; Schneider, S.; de Bruin, B. *Angew. Chem. Int. Ed.* **2014**, *53*, 6814-6818.
[30] Scepaniak, J. J.; Margarit, C. G.; Harvey, J. N.; Smith, J. M. *Inorg. Chem.* **2011**, *50*, 9508-9517.
[31] Klopsch, I.; Kinauer, M.; Finger, M.; Würtele, C.; Schneider, S. *Angew. Chem. Int. Ed.* **2016**, *55*, 4786-4789.
[32] Semproni, S. P.; McNeil, W. S.; Baillie, R. A.; Patrick, B. O.; Campana, C. F.; Legzdins, P. *Organometallics* **2010**, *29*, 867-875.
[33] Berry, J. F. *Comm. Inorg. Chem.* **2009**, *30*, 28-66.
[34] Anhaus, J. T.; Kee, T. P.; Schofield, M. H.; Schrock, R. R. *J. Am. Chem. Soc.* **1990**, *112*, 1642-1643.
[35] (a) Huynh, M. H. V.; White, P. S.; Meyer, T. J. *Angew. Chem., Int. Ed.* **2000**, *39*, 4101-4104. (b) Huynh, M. H. V.; El-Samanody, E.-S.; Demadis, K. D.; White, P. S.; Meyer, T. J. *Inorg. Chem.* **2000**, *39*, 3075-3085. (c) Huynh, M. H. V.; White, P. S.; Carter, C. A.; Meyer, T. J. *Angew. Chem. Int. Ed.* **2001**, *40*, 3037-3039. (d) Huynh, M. H. V.; Baker, R. T.; Jameson, D. L.; Labouriau, A.; Meyer, T. J. *J. Am. Chem. Soc.* **2002**, *124*, 4580-4582.

[36] (a) Brown, S. N. *J. Am. Chem. Soc.* **1999**, *121*, 9752-9753. (b) Man, W.-L.; Lam, W. W. Y.; Lau, T.-C. *Acc. Chem. Res.* **2014**, *47*, 427-439.
[37] Glüer, A.; Askevold, B.; Schluschaß, B.; Heinemann, F. W.; Schneider, S. *Z. Anorg. Allg. Chem.* **2015**, *641*, 49-51.
[38] (a) Rossi, G.; Gardini, M.: Pennesi, G.; Ercolani, C.; Goedken, V. L. J. *Chem. Soc., Dalton Trans.* **1989**, 193-195. (b) Bonomo, L.; Solari, E.; Scopelliti, R.; Floriani, C. *Angew. Chem. Int. Ed.* **2001**, *40*, 2529-2531.
[39] Given, K. W.; Pignolet, L. H. *Inorg. Chem.* **1977**, *16*, 2982-2984.
[40] Brookhart, M.; Grant, B.; Volpe, A. F. *Organometallics* **1992**, *11*, 3920-3922.
[41] Ivancic, I. *Water Res.* **1984**, *18*, 1143-1147.
[42] SAINT 7.68A, Bruker AXS Inst. Inc., WI, USA, Madison, **2009**.
[43] SADABS 2.06, Bruker AXS Inc., Madison, WI, USA, **2002**.
[44] SHELXTL NT 6.12, Bruker AXS Inc., Madison, WI, USA, **2002**.
[45] Neese, F. The ORCA program system. *Wiley Interdisciplinary Reviews: Computational Molecular Science* **2012**, *2*, 73-78.
[46] Perdew, J. P.; Burke, K.; Ernzerhof, M. *Phys. Rev. Lett.* **1996**, *77*, 3865-3868.
[47] Perdew, J. P.; Burke, K.; Ernzerhof, M. *J. Chem. Phys.* **1996**, *105*, 9982-9985.
[48] Weigend, F.; Ahlrichs, R. *Phys. Chem. Chem. Phys* **2005**, *7*, 3297-3305.
[49] Andrae, D.; Häussermann, U.; Dolg, M.; Stoll, H.; Preuss, H. *Theor. Chim. Acta* **1990**, *77*, 123-141.
[50] (a) Treutler, O.; Ahlrichs, R. *J. Chem. Phys.* **1995**, *102*, 346-354. (b) *Chem. Phys. Lett.* **1995**, *240*, 283-290. (c) *Chem. Phys. Lett.* **1995**, *242*, 652-660. (d) Eichkorn, K.; Weigend, F.; Treutler, O.; Ahlrichs, R. *Theo. Chem. Acc.* **1997**, *97*, 119-124.
[51] (a) Grimme, S.; Ehrlich, S.; Goerigk, L. *J. Comput. Chem.* **2011**, *32*, 1456-1465. (b) Grimme, S.; Antony, J.; Ehrlich, S.; Krieg, H. *J. Chem. Phys.* **2010**, *132*, 154104-154119.
[52] NBO 6.0. Glendening, E. D.; Badenhoop, J. K.; Reed, A. E.; Carpenter, J. E.; Bohmann, J. A.; Morales, C. M.; Landis, C. R.; Weinhold, F. Theoretical Chemistry Institute, University of Wisconsin, Madison (**2013**).
[53] Hanwell, M. D.; Curtis, D. E.; Lonie, D. C.; Vandermeersch, T.; Zurek, E.; Hutchison, G. R. *J. Cheminform.* **2012**, *4*, 17.
[54] Pettersen, E. F.; Goddard, T. D.; Huang, C. C.; Couch, G. S.; Greenblatt, D. M.; Meng, E. C.; Ferrin, T. E. *J. Comput. Chem.* **2004**, *25*, 1605-1612.
[55] Jmol: an open-source Java viewer for chemical structures in 3D. http://www.jmol.org/.

For Table of Contents use only

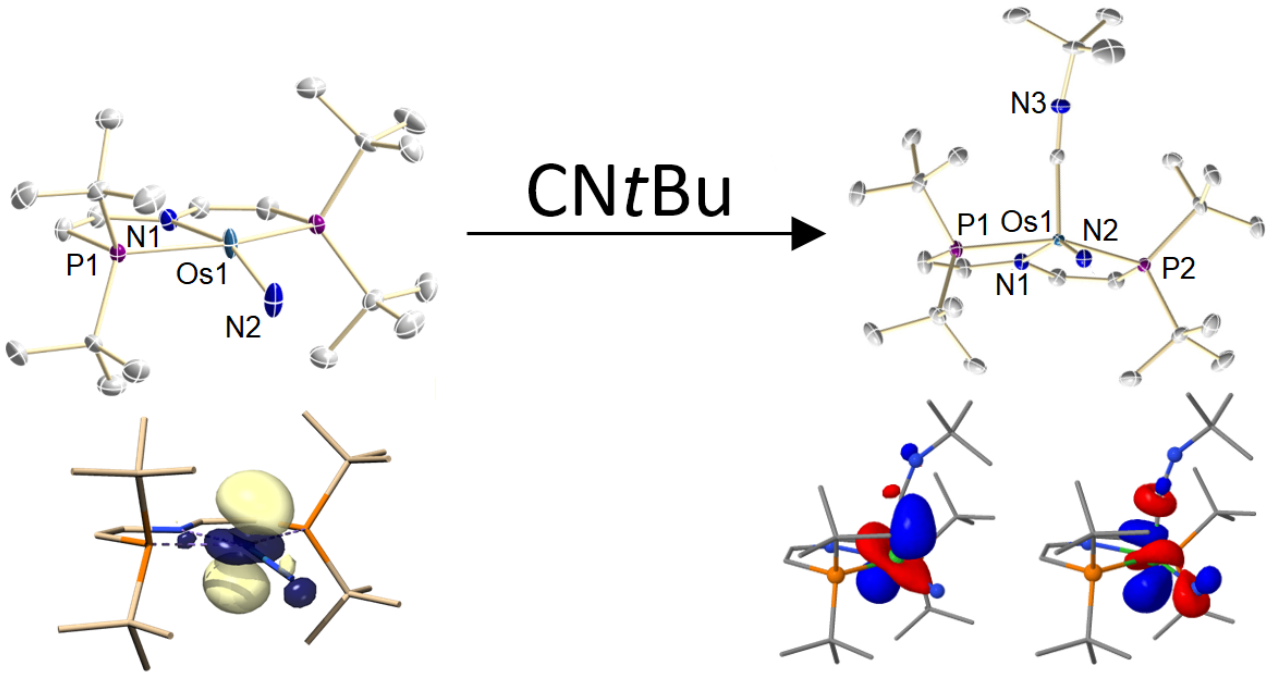

Four- and Five-coordinate Osmium(IV) Nitrides and Imides: Circumventing the 'Nitrido-Wall'

Josh Abbenseth[a], Sarah C. Bete[a], Markus Finger[a], Christian Volkmann[a], Christian Würtele[a], Sven Schneider[a]*

a. Institut für Anorganische Chemie, Georg-August-Universität Göttingen, Tammannstraße 4, 37077 Göttingen.

Sven.Schneider@chemie.uni-goettingen.de